ARTICLE IN PRESS

Polyhedron xxx (2017) xxx–xxx

Contents lists available at ScienceDirect

Polyhedron

journal homepage: www.elsevier.com/locate/poly

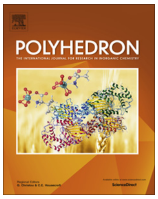

Iron and ruthenium complexes having a pincer-type ligand with two protic amidepyrazole arms: Structures and catalytic application

Yoshiko Nakahara [a], Tatsuro Toda [a], Shigeki Kuwata [a,b,*]

[a] Department of Chemical Science and Engineering, School of Materials and Chemical Technology, Tokyo Institute of Technology, 2-12-1 E4-1 O-okayama, Meguro-ku, Tokyo 152-8552, Japan
[b] PRESTO, Japan Science and Technology Agency (JST), 4-1-8 Honcho, Kawaguchi, Saitama 332-0012, Japan

ARTICLE INFO

Article history:
Received 12 July 2017
Accepted 30 August 2017
Available online xxxx

Keywords:
Pincer ligand
Pyrazole
Iron
Ruthenium
Hydrogen bond

ABSTRACT

This paper describes the iron and ruthenium complexes ligated by 2,6-di(5-pivalamido-1*H*-pyrazol-3-yl)pyridine (amide-LH_2) bearing electron-withdrawing $NHCOBu^t$ groups on the two protic pyrazole arms. Treatment of $FeCl_2{\cdot}4H_2O$ with an equimolar amount of amide-LH_2 followed by addition of two trimethylphosphine and an excess of sodium triflate gave the pincer-type iron complex $[Fe(MeCN)(\text{amide-}LH_2)(PMe_3)_2](OTf)_2$ (**1b**; OTf = OSO_2CF_3). Impact of the amido groups in **1b** on the reactions with hydrazines was evaluated. Complex **1b** catalyzed disproportionation of hydrazine into ammonia and dinitrogen, although the catalytic activity was lower than that of the Bu^t-LH_2 analogue **1a**. X-ray analysis of **1b** as well as the ruthenium complex $[\{RuCl_2(PPh_3)_2\}_2(\mu_2\text{-amide-}LH_2)_2]$ (**2b**) revealed that the pendant carboxamide groups along with the pyrazole NH units are engaged in hydrogen bonds in the second coordination sphere.

1. Introduction

Multiproton-responsive chelate ligands have attracted much attention owing to their versatile roles in mimicking the active sites of metalloenzymes and developing functional materials [1–4]. Among such scaffolds, 2,6-di(pyrazol-3-yl)pyridines (R-LH_2; Chart 1) with a variety of substituents R in the two protic pyrazole arms are easily accessed by conventional condensation reactions [5]. These ligands thus have been widely used as templates for catalysts [4,6–14], supramolecular architecture [15–18], and spin-crossover compounds [19] as well as photo-emitting and sensitizing complexes [20–22]. Despite of the structural diversity, however, the substituent effect on the reactivity of this class of compounds have scarcely been investigated [8].

Our continuing study on metal–ligand bifunctional complexes [4,7,23–26] led to the finding that the protic pincer-type iron complex $[Fe(MeCN)(Bu^t\text{-}LH_2)(PMe_3)_2](OTf)_2$ (**1a**) catalyzes disproportionation of hydrazine into dinitrogen and ammonia [6]. The reactions using N-methylated analogous catalysts as well as substituted hydrazines suggest that proton–electron shuttling between the $Fe(Bu^t\text{-}LH_2)$ fragment and substrate hydrazine molecule is operative. Given the mechanism, the Brønsted acidity of the pyrazole arms would greatly affect the catalytic performance. In this regard, the amide-LH_2 ligand recently developed by Halcrow and co-workers [27] is attractive since the electron-withdrawing nature of the amide group would facilitate proton transfer from the pincer ligand to the substrate molecule. We describe here the synthesis and catalysis of the iron complexes $[Fe(MeCN)(\text{amide-}LH_2)(PMe_3)_2](OTf)_2$ (**1b**). The crystal structure of a related ruthenium complex bearing the amide-LH_2 ligand, $[\{RuCl_2(PPh_3)_2\}_2(\mu_2\text{-amide-}LH_2)_2]$ (**2b**), is also reported.

2. Experimental

2.1. General

All manipulations were performed under an atmosphere of argon using standard Schlenk techniques unless otherwise specified. Solvents were dried by refluxing over sodium benzophenone ketyl (THF, diethyl ether, and hexane), P_2O_5 (dichloromethane and acetonitrile), and $Mg(OMe)_2$ (methanol), and distilled before use. 2,6-Di(5-pivalamido-1*H*-pyrazol-3-yl)pyridine (amide-LH_2) [27] and complex **2b** [8] as well as $[RuCl_2(PPh_3)_3]$ [28] were prepared according to the literature. ^1H (399.8 MHz) and ^{31}P (161.8 MHz) NMR spectra were obtained on a JEOL JNM-ECX-400 spectrometer. ^1H NMR shifts are relative to the residual CD_2HCN

---

[*] Corresponding author at: Department of Chemical Science and Engineering, School of Materials and Chemical Technology, Tokyo Institute of Technology, 2-12-1 E4-1 O-okayama, Meguro-ku, Tokyo 152-8552, Japan.

E-mail address: skuwata@apc.titech.ac.jp (S. Kuwata).

http://dx.doi.org/10.1016/j.poly.2017.08.044
0277-5387/© 2017 Elsevier Ltd. All rights reserved.

Please cite this article in press as: Y. Nakahara et al., Polyhedron (2017), http://dx.doi.org/10.1016/j.poly.2017.08.044

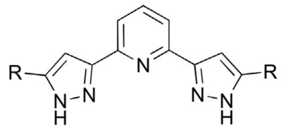

R-LH$_2$

Bu^t-LH$_2$: R = Bu^t
amide-LH$_2$: R = NHCOBu^t
H-LH$_2$: R = H

Chart 1.

(δ 1.93) and CHCl$_3$ (δ 7.26), while ^{31}P shifts are referenced to phosphoric acid (δ 0.0), respectively. *J* values are given in Hz. Infrared spectra were recorded on a JASCO FT/IR-6100 spectrometer. ESI-MS spectra was obtained on a JEOL JMS-T100LC (methanol was used as a solvent). UV–Vis spectra were recorded on a JASCO V-630 spectrometer. Nitrogen gas evolved in disproportionation of hydrazine was determined by GLC analysis using Shimadzu GC-2010 Plus gas chromatograph equipped with a Molecular Sieve 5A column. Elemental analyses were performed on a Perkin–Elmer 2400II CHN analyzer.

2.2. Synthesis of [Fe(MeCN)(amide-LH$_2$)(PMe$_3$)$_2$](OTf)$_2$ (**1b**)

A mixture of FeCl$_2$·4H$_2$O (19.2 mg, 0.0966 mmol) and amide-LH$_2$ (41.3 mg, 0.101 mmol) in methanol (4 mL) was stirred for 4 h at room temperature. Slow addition of diethyl ether (20 mL) afforded an orange solid, which is tentatively assigned as [FeCl$_2$(MeOH)(amide-LH$_2$)] (22.0 mg, 0.0387 mmol). ESI-MS: *m*/*z* 500.0 [FeCl(amide-LH$_2$)$^+$]. The solid was dissolved in acetonitrile (2 mL), and sodium trifluoromethanesulfonate (65.5 mg, 0.381 mmol) and a 1.0 M toluene solution of trimethylphosphine (0.08 mL, 0.08 mmol) were added. After stirring for 8 h at room temperature, the solvent was removed in vacuo. The residue was extracted with dichloromethane (5 mL). Slow addition of hexane (20 mL) to the concentrated extract (to ca. 1.5 mL) afforded black crystals, which were washed with diethyl ether (5 mL × 2). Yield: 15.0 mg (0.0157 mmol, 16% in two steps). ^{1}H NMR (CD$_3$CN): δ 0.70 (t, 18H, J_{PH} = 4.0, PMe$_3$), 1.25 (s, 18H, CMe$_3$), 6.91 (s, 2H, pyrazole CH), 7.96 (d, 2H, $^3J_{HH}$ = 8.3, 3- and 5-C$_5$H$_3$N), 8.07 (m, 1H, 4-C$_5$H$_3$N), 9.10 (s, 2H, amide NH), 11.79 (s, 2H, pyrazole NH). ^{31}P{^{1}H} NMR (CD$_3$CN): δ 17.7 (s). IR (KBr): 1699 cm^{-1} (C=O). *Anal.* Calc. for $C_{31}H_{48}F_6FeN_8O_8S_2P_2$: C, 38.92; H, 5.06; N, 11.71. Found: C, 38.83; H, 5.17; N, 11.71%.

2.3. Synthesis of [{RuCl$_2$(PPh$_3$)$_2$}$_2$(μ-amide-LH$_2$)$_2$] (**2b**)

A mixture of [RuCl$_2$(PPh$_3$)$_3$] (166.8 mg, 0.1740 mmol) and amide-LH$_2$ (68.8 mg, 0.168 mmol) in dichloromethane (10 mL) was stirred for 16 h at room temperature. After removal of the solvent, recrystallization from THF–hexane (5 mL/15 mL) afforded **2b**·2THF·hexane as red crystals. The thoroughly dried sample was found to lose the solvating molecules on the basis of ^{1}H NMR spectroscopy and combustion analysis. Yield: 156.8 mg (0.07088 mmol, 84%). ^{1}H NMR (CDCl$_3$): δ 1.18 (s, 36H, CMe$_3$), 6.91 (t, 24H, *J* = 7.5, PPh$_3$), 7.04 (d, 4H, $^4J_{HH}$ = 2.2, pyrazole CH), 7.13 (t, 12H, J_{HH} = 7.0, PPh$_3$), 7.21 (d, 4H, $^3J_{HH}$ = 7.7, 3- and 5-C$_5$H$_3$N), 7.30–7.34 (m, 24H, PPh$_3$), 7.59 (t, 2H, $^3J_{HH}$ = 8.0, 4-C$_5$H$_3$N), 10.33 (br s, 4H, NH), 12.41 (br d, 4H, $^4J_{HH}$ = 2.4, NH). ^{31}P{^{1}H} NMR (CDCl$_3$): δ 35.3 (s). IR (KBr): 1687 cm^{-1} (C=O). *Anal.* Calc. for $C_{114}H_{114}Cl_4N_{14}O_4P_4Ru_2$: C, 61.90; H, 5.19; N, 8.86. Found: C, 62.18; H, 5.44; N, 8.51%.

2.4. Representative procedure for catalytic disproportionation of hydrazine wtih **1**

To a dichloromethane–methanol (1 mL/1 mL) solution of **1b** (9.2 mg, 0.0096 mmol) in a Schlenk tube (inside volume: ca. 33 mL) was added anhydrous hydrazine (6.1 μL, 0.19 mmol), and the mixture was stirred for 18 h at room temperature. An aliquot (1 mL) of the gas phase was subjected to GLC analysis. The NMR analysis with using 1,3,5-trimethoxybenzene as an internal standard suggested formation of a hydrazinophosphonium triflate, (Me$_3$PNHNH$_2$)OTf, in 23% yield. ^{1}H NMR (CDCl$_3$): δ 1.97 (d, 9H, $^2J_{PH}$ = 13.1, PMe$_3$). ^{31}P{^{1}H} NMR (CDCl$_3$): δ 50.3 (s). This phosphonium salt was not detected in the reaction of **1a**. In a separate run, all volatile material inside was distilled into a 1 N H$_2$SO$_4$ aqueous solution after the reaction, and the residue was further extracted with an additional amount of distilled water. The collected ammonia and unreacted hydrazine were quantified by indophenol [29] and *p*-(dimethylamino)benzaldehyde method [30], respectively.

2.5. Representative procedure for the reaction of **1** with 1,1-diphenylhydrazine

To a solution of **1b** (1.6 mg, 0.0017 mmol) in CD$_2$Cl$_2$ (0.5 mL) in an NMR tube were added Ph$_2$NNH$_2$ (1.4 μL, 0.0085 mmol) and 1,3,5-trimethoxybenzene (0.5 mg, 0.003 mmol) as an internal standard at room temperature. After 18 h, the mixture was subjected to ^{1}H NMR analysis.

2.6. Crystallography

Single crystals suitable for X-ray analyses were mounted on a fiber loop. Diffraction experiments were performed on a Rigaku Saturn CCD area detector with graphite monochromated Mo Kα radiation (λ = 0.710 70 Å). Intensity data were corrected for Lorentz–polarization effects and for absorption. Intensity data (6° < 2θ < 55°) were corrected for Lorentz–polarization effects and for absorption. Details of crystal and data collection parameters are summarized in Table 1. Structure solution and refinements were carried out by using the CrystalStructure program package [31]. The heavy-atom positions were determined by a direct methods program (SIR92 [32]) and the remaining non-hydrogen atoms were found by subsequent Fourier syntheses and refined by full-matrix least-squares techniques against F^2 using the SHELXL-2014/7 program [33]. One of the *tert*-butyl groups in **1b** was placed at two disordered positions with 65% and 35% occupancies and

Table 1
Crystal data for **1b** and **2b**·2THF·hexane.

	1b	**2b**·2THF·hexane
Formula	$C_{31}H_{48}F_6FeN_8O_8P_2S_2$	$C_{128}H_{144}Cl_4N_{14}O_6P_4Ru_2$
M	956.67	2442.48
Cryst. system	orthorhombic	monoclinic
Space group	*Pbcn*	*P*2$_1$/*n*
a (Å)	41.556(14)	26.295(7)
b (Å)	11.028(4)	14.963(4)
c (Å)	19.136(6)	30.494(8)
α (°)	90	90
β (°)	90	99.282(3)
γ (°)	90	90
V (Å^3)	8770(5)	11841(5)
T (K)	93	93
Z	8	4
μ (Mo Kα) (mm^{-1})	0.591	0.461
D_{calc} (g cm^{-3})	1.449	1.370
Limiting indices	$-53 \le h \le 53$	$-34 \le h \le 33$
	$-14 \le k \le 14$	$-19 \le k \le 19$
	$-24 \le l \le 24$	$-39 \le l \le 39$
No. of unique reflection	9407	27062
R_{int}	0.0547	0.1125
No. variables	551	1396
R_1 [$I > 2\sigma(I)$]	0.0800	0.0919
wR_2 (all data)	0.2263	0.1841
Goodness of fit (GOF) on F^2	1.140	1.180

Please cite this article in press as: Y. Nakahara et al., Polyhedron (2017), http://dx.doi.org/10.1016/j.poly.2017.08.044